

MINERALOGICAL AND PETROGRAPHIC ANALYSIS OF KASIYA FLAKE GRAPHITE ORE

CHRISTOPHER NGWENYA

(ESC/025/20)

THYOLO, MALAWI

DISSERTATION SUBMITTED TO NDATA SCHOOL OF CLIMATE AND EARTH SCIENCES OF THE MALAWI UNIVERSITY OF SCIENCE AND TECHNOLOGY IN PARTIAL FULFILLMENT OF THE REQUIREMENTS FOR THE AWARD OF BACHELOR OF SCIENCE DEGREE IN EARTH SCIENCES (GEOLOGY)

05 May, 2025

DISSERTATION APPROVED BY:

SUPERVISORS:

MR T SHABA: Signature:_____ T. Shaba _____

CO-SUPERVISORS:

MR ANDRIES: Signature:_____

(SSL Technical Manager)

DECLARATION

I, Christopher Ngwenya, declare that the work in this dissertation titled "Mineralogical And Petrographic Analysis on Kasiya Flake Graphite Ore" has been carried out by me. All information retrieved from other literature has been acknowledged in the text and a list of references provided. I declare to have used AI tools to modify grammar.

Signature:_____

DISCLAMER

This document outlines work conducted in partial fulfillment of academic requirements at the Ndata School of Climate and Earth Sciences, Malawi University of Science and Technology. The views and opinions expressed herein are solely those of the author(s) and do not necessarily reflect the official position or policies of the School.

ABSTRACT

This study presents a comprehensive mineralogical and petrographic investigation of flake graphite from the Kasiya deposit, integrating thin section microscopy, X-ray fluorescence (XRF), Inductively coupled plasma-optical emission spectrometry (ICP-OES), and general chemical analysis. Petrographic analysis revealed a mineral assemblage dominated by graphite, quartz, feldspar, muscovite and chlorite, with graphite occurring as a disseminated flakes aligned along foliated planes. Textural features such as recrystallized quartz mosaics and chlorite overgrowths provide compelling evidence for metasomatic alteration. Elemental geochemical data highlight the presence of mobile ions such as Fe, Al, Na, Ca, and K, further confirming fluid-driven metasomatic processes. This study also established a correlation between graphite flake size and grade, with samples exhibiting large flakes corresponding to higher graphite concentrations. The origin of metasomatism is interpreted to be associated with CO_2- and H_2O-rich metamorphic fluids, possibly linked to regional tectonothermal events. These findings enhance the formation mechanism of graphite in high-grade metamorphic terranes and provides valuable insights for resource evaluation and beneficiation strategies.

ACKNOWLEDGEMENT

The completion of this dissertation marks the culmination of an intensely challenging yet profoundly transformative chapter in my academic journey. While the path demanded relentless perseverance, it has been illuminated by the unwavering support of mentors, institutions, and loved ones to whom I owe immeasurable gratitude.

First and eternally, I acknowledge the divine grace of Almighty God, whose boundless wisdom and faithfulness sustained me through every season of this four-year odyssey—moments of confident strides, weary trudges, and even uncertain crawls. His presence, a constant companionship surpassing earthly bonds, guided me through the intellectual and emotional complexities of this research. To Him alone be all glory, now and forever.

My profound thanks extend to my academic advisors, Mr. T. Shaba and Miss E Nsamila, whose intellectual rigor and patient mentorship shaped the scholarly foundations of this work. Beyond refining methodologies, they nurtured my growth as a critical thinker, challenging me to bridge theoretical frameworks with real-world applicability. Their timely feedback and steadfast belief in this project's potential were anchors during moments of uncertainty.

I extend my deepest appreciation to Sovereign Services Limited for their steadfast commitment to advancing scholarly inquiry, exemplified by their willingness to host this research within their operational framework and their generous financial sponsorship of this project. Their trust in academic collaboration has been instrumental in bridging theoretical knowledge with industry practice, creating a model for impactful public-private partnerships in research. A special note of gratitude is reserved for Mr. Andries Kruger, Technical Manager, whose expertise, mentorship, and dedicated oversight elevated every phase of this undertaking. From troubleshooting logistical hurdles to providing critical technical insights, his proactive engagement ensured the project's rigor and relevance. His willingness to share institutional knowledge and advocate for resource access exemplified professionalism at its finest.

To both Sovereign Services Limited and Mr. Kruger, this work stands as a testament to the transformative power of institutional support and individual generosity in scholarly pursuits

To my colleagues and peers, thank you for the vibrant debates, candid critiques, and shared laughter that transformed isolation into camaraderie. Your perspectives sharpened my arguments and reminded me that intellectual growth thrives in community.

My mother, Emily Banda, remains my bedrock. Her unwavering belief in my potential, even when my own faltered, provided the emotional resilience to persist. This milestone is as much hers as it is mine.

Finally, to Pempho Nsambati, my partner in every sense, I owe debts beyond words. Her financial sacrifices, emotional fortitude, and intellectual encouragement not only fueled my determination but redefined the meaning of partnership. This work is a testament to her enduring love and faith in my dreams.

TABLE OF CONTENT

Contents

ABSTRACT 5

ACKNOWLEDGEMENT 6

CHAPTER 1: INTRODUCTION 10

1.1: BACKGROUND 10

1.2 : PROBLEM STATEMENT 13

1.3: RESEARCH OBJECTIVES 14

1.31: MAIN OBJECTIVE 14

1.32: SPECIFIC OBJECTIVES 14

1.4: RESEARCH QUESTIONS 14

1.5: SIGNIFICANCE OF STUDY 14

CHAPTER 2: LITERATURE REVIEW 15

2.10: THE GEOLOGY 18

2.11 REGIONAL GEOLOGY 18

CHAPTER 2.20: REGIONAL GEOLOGY 20

CHAPTER 3: METHODOLOGY 22

3.1: DESK STUDY 23

3.2: FIELD WORK AND SAMPLING 23

3.21. Step 1: mapping 23

3.22. Step 2: sampling strategy 25

3.3 SAMPLE PREPARATION 27

3.31. Sample crushing and drying 28

3.32. Sample composing 28

3.33. Sample Screening 28

3.34. Desliming 28

3.35. **Froth Flotation samples** 29

3.4. LABORATORY TECHNIQUES 30

3.41. Froth Flotation 30

3.42. Petrography 31

3.43 Steps in Thin Sectioning 32

3.44. Mineralogical characteristics 32

3.5 Geochemical Analysis 33
3.51. X-Ray Fluorescence (XRF) 33
3.52. Inductively Coupled Plasma Mass Spectrometry (ICP-OES) 33
CHAPTER 4: RESULTS AND DISCUSION 33
4.1. Petrography 33
4.1.1 thin sections 33
4.12 Common Flake Morphology 35
4.13 Overview of Thin Sections 36
4.14 Petrographic interpretation 36
4.15 Flake Size Distribution 37
4.2 X-Ray Fluorescence XRF Results 38
4.21 Mineralization process 38
4.22 Metasomatic Influences 39
4.23 Major Elements and Host Matrix 40
4.24 Accessary/Trace Elements 40
4.25 Petro-genetic Implications 41
4.26 Mineralogical Indicators (Inferred from XRF) 41
4.27 Implications for Beneficiation 41
4.3 ICP-OES 41
4.31 Metasomatic Activity 43
CHAPTER 5: CONCLUSION AND RECOMMENDATIONS 44
5.1 CONCLUSION 44
5.2 RECOMMENDATION 45
REFERENCES 46

CHAPTER 1: INTRODUCTION

1.1: BACKGROUND

Graphite is the most stable allotrope of carbon at room temperature and atmospheric pressure (Puronaho, 2018). Its atomic arrangement of hexagonal sheets, bound by weak van der Waals forces, imparts perfect cleavage, extreme softness, and a greasy feel (Meunier, 2015). It also has an exceptionally high melting point of 3550°C (Mitchell, 1993). Graphite can be naturally sourced or synthetically produced, catering to diverse industrial demands (Robinson et al.,2017). Natural graphite exhibits exceptional properties, which are closely tied to its electronic and crystal structure-property relationship. It has a density of $\rho = 2.26$ g/cm³, and the anisotropic conductivity ratio σ ranges between 10^2 and 10^4 in single-crystal graphite, reflecting its highly directional electrical conductivity (Zhu et al., 2019; Smith, 2020). The material has an average compressibility $\beta = 3.10 \times 10^{11}$ N/m², a shear modulus $\tau = 2.30 \times 10^9$ N/m², and an impressive Young's modulus $E = 1.13 \times 10^{14}$ N/m², making it one of the stiffest materials known (Lee & Kim, 2021). Additionally, graphite's surface energy $\gamma = 0.12$ J/m² and sublimation point, ranging from $T = 4000$ to 4200 K, further highlight its thermal stability and mechanical resilience (Jones, 2018).

These exceptional attributes, particularly its non-metallic characteristics, have historically enabled a wide range of traditional applications. For instance, graphite is indispensable in the production of refractories, lubricants, brake linings, pencils, paints, crucibles, coatings, and gaskets (Brown et al., 2016). Beyond these, graphite's metallic conductivity and exceptional thermal properties have positioned it as a cornerstone material in modern industries. Emerging applications include its use in fuel cells, Li-ion batteries, nuclear energy systems, thermal energy storage, consumer electronics, graphene production, and water purification technologies (Johnson & Walker, 2022; Patel et al., 2023).

Among the various types of graphite, flake graphite is particularly sought after due to its high purity and suitability for high-tech applications. The growing demand for flake graphite, driven by the global transition to clean energy and electric vehicles, has heightened interest in exploring and characterizing graphite deposits worldwide. The increasing global demand for natural graphite, driven by its crucial role in green energy transition, particularly for use in battery anodes

in lithium-ion batteries, stationary batteries, lead-acid batteries, and fuel cells, has underlined the need to identify and explore new sources of natural graphite (Statista.,2024). Recognizing its importance, several countries, including the United States, China, India, and the European Union, have listed natural graphite as a critical mineral.

In Europe, countries such as Ukraine, Austria, and Sweden are notable for their graphite production, with Ukraine holding significant reserves (European Minerals Yearbook, 2023). In America, countries like Brazil, Mexico, and Canada are key players. Brazil, in particular, has emerged as a major producer, with substantial reserves second only to China. Mexico is recognized for its production of amorphous and flake graphite (US Geological Survey, 2023). In Asia, leading producers include China, India, Sri Lanka, Japan, and South Korea, with China being the largest global producer, contributing over 75% of the world's graphite production as of 2024 (Roskill, 2024). Sri Lanka is particularly renowned for its high-quality lump or vein graphite, while other Asian nations focus on flake graphite.

Africa is increasingly gaining attention for its graphite reserves and production potential. Madagascar and Mozambique are among the continent's leading producers, with Mozambique hosting one of the world's largest high-grade graphite deposits (International Energy Agency, 2024). Malawi is emerging as a significant player with the Kasiya Graphite Project, located in the Lilongwe Plain. This project, developed by Sovereign Metals Limited, is recognized as the second-largest flake graphite deposit globally and is projected to produce approximately 244,000 tonnes of graphite annually. The Kasiya Project is also notable for its environmentally sustainable mining practices and its potential to contribute significantly to the global graphite supply chain, particularly for applications in energy storage and electric vehicles (Sovereign Metals, 2025).

Other African nations, including Tanzania, Namibia, South Africa, and Uganda, are known to have significant graphite reserves, with Tanzania's Nachu Project and Mozambique's Balama Mine being prominent examples. These reserves position Africa as a critical player in meeting the growing global demand for graphite, particularly for applications in electric vehicle batteries and energy storage (World Bank Group, 2023)

Africa hosts world-class graphite deposits, including Mozambique's Balama (Syrah resources) and Tanzania's Nachu (Magnis Energy). The unique characteristics of graphite deposits vary by region, influencing their suitability for specific applications. For instance, flake graphite from Madagascar, Mozambique, and Malawi is highly sought after for its purity and quality. In Malawi, part of the East Africa Orogen, has recently emerged as a graphite hotspot, with Kasiya deposit ranked as the second-largest flake graphite resource globally (Sovereign Metals,2023). As global demand for graphite continues to rise, particularly in emerging technologies, these regions are expected to play an increasingly vital role in the graphite supply chain.

Malawi's geology is dominated by the Ubendian belt, a paleoproterozoic to Neoproterozoic metamorphic terrane formed during the assembly of Gondwana supercontinent (Vrana et al.,2004). The Kasiya deposit is located in central Malawi, containing an estimated 211 million tonnes of graphite at 8.6% total graphitic carbon (TGC)(Sovereign Metals, 2023). The preliminary reports suggest a metamorphic origin, but detailed mineralogical and genetic studies are lacking. Given the importance of graphite in meeting global green energy goals, this study focuses on Kasiya's flake graphite mineralogy and petrography.

Although Malawi hosts the second-largest flake graphite deposit in the world, there remains a significant gap in comprehensive studies focusing on the mineralogical and petrographic characteristics of its graphite ore. The Kasiya deposit, located in the Lilongwe District, is particularly notable for its high-grade flake graphite, which is essential for various industrial applications, including the production of lithium-ion batteries and other green energy technologies (Sovereign Metals Limited, 2024). Despite its global significance, detailed scientific investigations into the mineralogical and petrographic properties of the Kasiya flake graphite are lacking. This study, therefore, represents the first systematic effort to analyze the petrographic and mineralogical composition of the Kasiya flake graphite, aiming to provide critical insights into its quality, formation, and potential applications.

1.2 : PROBLEM STATEMENT

The continued global reliance on petroleum as a primary energy source has led to increasingly evident negative environmental impacts, including significant pollution, greenhouse gas emissions, and the depletion of finite natural resources. These challenges emphasize the urgent need for sustainable alternatives (International Energy Agency [IEA], 2023). Transitioning to renewable energy sources and advanced technologies has become a global priority, with critical minerals playing a pivotal role in this shift (Doe,2020).

Among these minerals, flake graphite is indispensable due to its vital applications in lithium-ion batteries, fuel cells, and composite materials, making it integral to energy storage systems and the advancement of electric vehicles (Roskill, 2024). Recently, Malawi's Kasiya deposit, identified as one of the world's largest pre-developed flake graphite resources, has emerged as a critical opportunity to support not only Malawi's economic development but also the global transition to green technologies (Sovereign Metals, 2025). However, despite its significance, the Kasiya deposit on-study. A limited published data on its mineralogical composition, petrographic characteristics, and geological genesis presents a challenge to its full industrial utilization (World Bank Group, 2023).

Furthermore, there are knowledge gaps regarding key properties such as flake size distribution, crystallinity, and purity phases, which are crucial for evaluating its suitability for advanced industrial applications (US Geological Survey [USGS], 2023). An unresolved question pertains to the role of metamorphic versus hydrothermal processes in the deposit's graphite formation, impacting resource extraction strategies and efficiency (Lee et al., 2022). These deficiencies in understanding contribute to uncertainties in ore heterogeneity, potentially leading to inefficient mining and processing. Consequently, Malawi risks losing competitiveness in the global graphite supply chain, especially as the demand for high-grade graphite continues to grow to meet the requirements of emerging green technologies (IEA, 2023).

Addressing these research gaps is essential to unlocking the full potential of the Kasiya graphite deposit. Comprehensive studies on its geological, mineralogical, and industrial properties are

necessary not only to enhance mining efficiency but also to position Malawi as a key player in the sustainable mineral economy and the global transition to renewable energy.

1.3: RESEARCH OBJECTIVES

1.31: MAIN OBJECTIVE

The objective was to analyze the mineralogical, petrographic, and geochemical characteristics of the Kasiya graphite deposit.

1.32: SPECIFIC OBJECTIVES

- To determine the mineralogical composition of the graphite ore.
- To characterize the flake size distribution.
- To analyze elemental impurities of the flake graphite ore.
- To analyze the metamorphic/metasomatic conditions that lead to graphite formation

1.4: RESEARCH QUESTIONS

This research will address the questions like:

1. What are the mineralogical characteristics of Kasiya flake graphite?

2. What are the petrographic characteristics of Kasiya graphite ore?

3. What geological processes controlled the formation of graphite at Kasiya?

4. How do mineralogical properties of Kasiya graphite influence its suitability for industrial application

5. what are the associated elemental impurities of the Kasiya flake graphite ore and hoe do they affect beneficiation.

1.5: SIGNIFICANCE OF STUDY

The study has a number of significances, some of which are advancing geological knowledge, economic impact for Malawi, industrial relevance, and global and regional development.

The study of the Kasiya graphite deposit advances geological knowledge by providing the first detailed mineralogical and petrographic analysis of this significant resource in Malawi's Precambrian belt. It examines critical attributes like flake size, crystallinity, and impurities to better understand the deposit's formation processes and enhance global models for graphite genesis. Moreover, the findings allow for comparisons with world-class deposits, such as Balama in Mozambique, positioning Kasiya as a potentially competitive source in the global graphite market. With rising demand for high-quality graphite in renewable energy and technology sectors, this research is instrumental in evaluating Kasiya's role in addressing global graphite supply needs.

Economically, the Kasiya deposit presents transformative opportunities for Malawi, a country striving to diversify its economy beyond agriculture. As one of the world's largest undeveloped flake graphite resources, Kasiya could establish Malawi as a significant player in the global graphite industry. Its development promises economic benefits through job creation, infrastructure improvements, and foreign investment while fostering regional trade partnerships. Additionally, the study emphasizes sustainable mining practices and efficient processing strategies to enhance the deposit's market competitiveness. By leveraging this resource, Malawi could support renewable energy innovations and achieve substantial socioeconomic progress

CHAPTER 2: LITERATURE REVIEW

Graphite, a naturally occurring crystalline form of carbon, predominantly forms in metamorphic and igneous rocks (Meunier, 2015). Graphite can be classified as either naturally occurring or produced synthetically (Robinson et al. 2017). Natural graphite is formed either syn-genetically or epigenetically (Bullock and Morgan 2015). Syngenetic graphite is formed by metamorphism of the preserved organic materials in the sediments (Rosing-Schow et al 2017). It results in two categories of graphite, namely crystalline flake graphite and microcrystalline or amorphous graphite (Mitchell 1993, Wissler 2006, Simandl et al. 2015) while epigenetic is formed by the precipitation of carbon from C-H-O fluids in the veins during retrograde metamorphism (Bullock and Morgan 2015, Simandl et al. 2015). Syngenetic vein type or lump graphite results from epigenetic processes (Puronaho, 2018). It exists in three commercial forms: crystalline lump or vein graphite, crystalline flake graphite, and microcrystalline or amorphous graphite (Palosaari et

al., 2020). At the atomic level, graphite's structure is characterized by carbon atoms arranged in hexagonal layers known as graphene, linked via covalent and metallic bonds through sp^2 hybridization (Mitchell, 1993). These graphene layers are bound by weak van der Waals forces, allowing them to slide effortlessly past each other, a unique feature responsible for graphite's exceptional properties, including softness, lubricity, and superior thermal and electrical conductivity (Simandl et al., 2015).

As a mineral, graphite is gray-black, opaque, soft (ranking 1–2 on the Mohs hardness scale), and exhibits a metallic luster along with a greasy feel (Puronaho, 2018). It has a low density (2.09–2.23 g/cm^3) and demonstrates remarkable resistance to thermal shock and high electrical conductivity. Additional physical traits include inertness, compressibility, elasticity, lubricity, and a specific gravity of approximately 2.2 (Palosaari et al., 2020). These properties enable graphite to serve both metallic and non-metallic functions, making it a versatile material for industrial applications.

Graphite is one of the most common naturally occurring solid forms of carbon. Its structure consists of hexagonal sheets with weak van der Waals forces holding the layers together. This unique arrangement gives graphite its perfect cleavage, resulting in its renowned softness and greasy texture (Meunier 2015, Palosaari et al. 2020). Graphite consists of numerous layers of parallel planar C6 rings, forming a polymorphic crystal structure that can be either hexagonal close-packed (HCP) or rhombohedral. The in-plane C-C bond length in these structures is 0.14 nm. Graphite can be categorized into three types based on its structural characteristics: crystalline flake, lump or vein, and amorphous. It's important to note that graphite and fullerene, which exhibit sp2 trigonal hybridization, form allotropes with cubic structural diamond, which displays sp3 tetrahedral hybridization (Qi Y, et al, 2019). Graphite is the most stable form of carbon at room temperature and atmospheric pressure (Puronaho, 2018). It exhibits both non- metallic and metallic properties and has a high melting point of 3550 °C (Mitchell, 1993; Simandl et al., 2015). Graphite can be categorized as either naturally occurring or synthetically produced (Robinson et al., 2017). Natural graphite can form through two processes: syn-genetically or epigenetically. Syngenetic graphite results from the metamorphism of organic materials preserved within sediments (Simandl et al., 2015, MUST,2020). Epigenetic graphite forms through the precipitation

of carbon from C-H-O fluids in veins during retrograde metamorphism (Bullock and Morgan, 2015;). Syngenetic graphite, on the other hand, results in two categories: crystalline flake graphite and microcrystalline (or amorphous) graphite (Simandl et al., 2015)

Graphite is one of the most abundant naturally occurring solid forms of carbon, characterized by its unique structure of hexagonal sheets held together by weak van der Waals forces. This arrangement imparts graphite with its perfect cleavage, softness, and greasy texture (Meunier, 2015; Palosaari et al., 2020). The polymorphic crystal structure of graphite can exist in two forms: hexagonal close-packed (HCP) and rhombohedral. The in-plane carbon-carbon (C-C) bond length in these structures is approximately 0.14 nm, contributing to its stability and unique properties.

Graphite is categorized into three structural types: crystalline flake, lump or vein, and amorphous. It is important to note that graphite and fullerene, which exhibit sp2 trigonal hybridization, form allotropes alongside cubic structural diamond, which displays sp3 tetrahedral hybridization (Qi et al., 2019). Among these, crystalline flake graphite is particularly valued for its high purity and crystallinity, making it suitable for advanced industrial applications such as lithium-ion batteries, lubricants, and refractories.

Graphite is the most stable form of carbon at room temperature and atmospheric pressure (Puronaho, 2018). It exhibits both metallic and non-metallic properties, including a high melting point of 3550 °C, excellent thermal and electrical conductivity, and chemical inertness (Mitchell, 1993; Simandl et al., 2015). Graphite can be classified as either naturally occurring or synthetically produced (Robinson et al., 2017). Natural graphite forms through two primary processes: syngenetic and epigenetic. Syngenetic graphite results from the metamorphism of organic materials preserved within sediments, while epigenetic graphite forms through the precipitation of carbon from C-H-O fluids in veins during retrograde metamorphism (Simandl et al., 2015; Bullock & Morgan, 2015).

The mineralogical and petrographic analysis of the Kasiya flake graphite deposit in Malawi provides critical insights into the genesis and quality of this resource. Syngenetic graphite, which dominates the Kasiya deposit, exhibits high purity and crystallinity, aligning with industrial specifications for high-performance applications. Recent studies have highlighted the significance

of Kasiya as the second-largest flake graphite deposit globally, with potential to meet the rising demand for graphite in renewable energy technologies and electric vehicles (Sovereign Metals, 2025).

Global natural graphite production reached approximately 1.6 million metric tons in 2024, with China accounting for over 75% of the total output, followed by Mozambique, Brazil, and Madagascar (Statista, 2025). However, the depletion of near-surface oxidized graphite deposits in China has led to export restrictions, creating supply pressures and emphasizing the importance of alternative sources like Kasiya (Rosing-Schow et al., 2017; Sunkari & Zango, 2018). The development of the Kasiya deposit not only addresses these supply challenges but also positions Malawi as a key player in the global graphite market

2.10: THE GEOLOGY

2.11 REGIONAL GEOLOGY

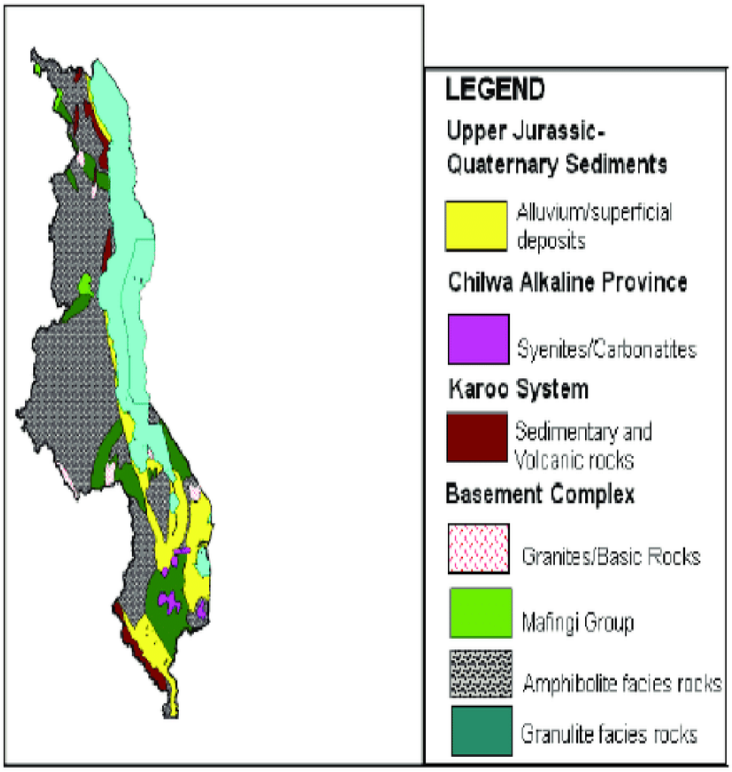


Figure1:(a) Geology of Malawi.

Malawi's geology is characterized by Precambrian basement rocks within the Ubendian Belt, part of the Mozambique Belt, which comprises Paleoproterozoic crystalline Basement Complex rocks subjected to high-grade metamorphism (De Waele et al., 2015). These rocks, including gneisses and schists, were shaped by tectonic collisions during the Archean and Proterozoic eons (Tsunogae et al., 2021). Overlying these basement rocks are sedimentary sequences of the Karoo Supergroup, deposited from the Late Carboniferous to Early Jurassic, which include sandstones, shales, and coal seams formed in glacial to fluvial environments (Britannica, n.d.). The region also features dolerite and basaltic intrusions linked to the Permo-Triassic magmatism during Gondwana's breakup (Jaeckel et al., 1997; Tsunogae et al., 2021).

Graphite mineralization is prevalent in Malawi's Precambrian metamorphic rocks, particularly within the Ubendian Belt, where tectonic and metamorphic processes concentrated carbon into economically significant deposits (De Waele et al., 2015). This geological diversity, encompassing tectonic, magmatic, and sedimentary processes, underscores Malawi's potential for mineral exploration, particularly for coal and graphite resources (De Waele et al., 2015; Tsunogae et al., 2021)

CHAPTER 2.20: REGIONAL GEOLOGY

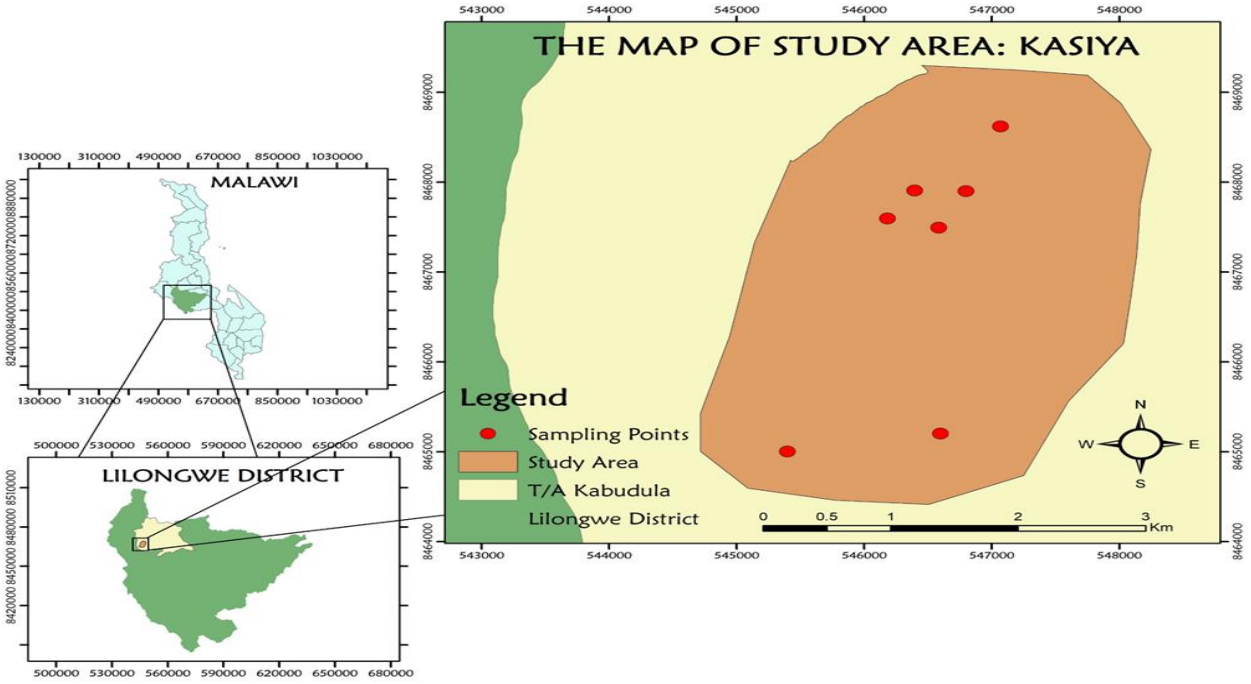


Figure 2. a. *the geology of Kasiya,* (Mchinji-upper Bua): *geology of Malawi,* GSD bulletin# 23

The geological framework of Lilongwe, Mchinji, and Upper Bua is primarily defined by the Precambrian Basement Complex, which consists of ancient metamorphic and igneous rocks that have undergone extensive deformation and weathering over millions of years (Bloomfield, 1965; Carter & Bennett, 1973). These regions form part of Malawi's cratonic shield, characterized by deep-seated metamorphism and magmatic intrusions associated with prolonged tectonic activity. The dominant rock types include gneisses, schists, and granites, which reflect a complex geological history involving tectonic compression, high-grade metamorphism, and episodic magmatism. Over time, prolonged weathering under tropical conditions has contributed to the formation of extensive lateritic profiles, particularly in Lilongwe and Upper Bua, where iron-rich soils and potential bauxite deposits are present (Freyberg, 1966). Furthermore, the influence of fluvial activity along river valleys, such as the Bua River, has resulted in the deposition of alluvial sediments, modifying the geomorphology of the region.

Lithologically, the region is predominantly composed of granitoid gneisses and schists, exhibiting varying degrees of foliation and deformation. The gneisses, widely exposed in Lilongwe and

Mchinji, are characterized by alternating bands of quartz, feldspar, and biotite, indicative of deep metamorphic origins (Carter & Bennett, 1973). In Mchinji, pegmatitic intrusions are present within the gneissic basement, containing feldspar, quartz, and, in some instances, lithium-bearing minerals or rare earth elements (Bloomfield, 1965). Schistose formations, more prevalent in Upper Bua, suggest medium-to high-grade metamorphism, often associated with tectonic shear zones (Freyberg, 1966). Additionally, dolerite dykes and other mafic intrusions, which cut across older rock units, provide evidence of past magmatic activity and may be linked to localized mineralization. Lateritic weathering has played a crucial role in modifying the lithology, especially in Lilongwe and Upper Bua, where deep oxidation has led to the enrichment of iron oxides and the formation of potentially economic bauxite deposits (Bloomfield, 1965).

The structural geology of the region has been significantly shaped by major tectonic events, particularly those linked to the East African Rift System (EARS) (Dixey, 1960). The rifting process has introduced faulting, folding, and extensive fracturing of the basement rocks, which have influenced groundwater movement and mineralization patterns. Major fault zones, primarily aligned along north-south and east-west orientations, serve as structural controls on rock deformation and fluid migration (Carter & Bennett, 1973). Shear zones, especially evident in Mchinji and Upper Bua, have facilitated hydrothermal activity, potentially contributing to localized mineral deposits such as graphite, heavy mineral sands, and pegmatite-hosted rare earth elements. In some areas, the presence of tightly folded schists and gneisses indicates a history of compressional forces associated with ancient orogenic events (Bloomfield, 1965). The fracturing of basement rocks has also enhanced groundwater recharge and storage, making these geological structures critical for hydrological studies and water resource management.

The Kasiya Rutile-Graphite deposit, located to the northwest of Malawi's capital city, Lilongwe, lies within the expansive Lilongwe Plain. This plain is characterized by flat to gently undulating topography, with its geology dominated by Precambrian basement rocks. These rocks include paragneiss with pelitic, psammitic, and calcareous units (Sovereign Metals, 2019). The paragneiss units are particularly significant as they host rich concentrations of both rutile and graphite, which are of great economic importance to Malawi's mining sector.

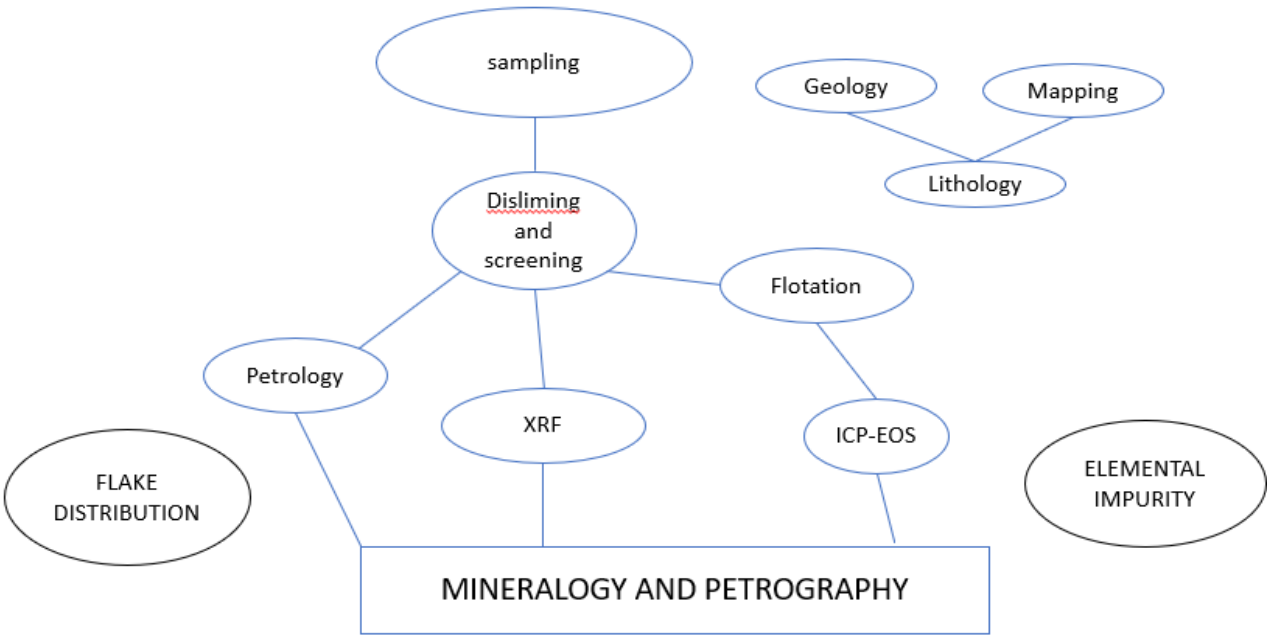
The high-grade rutile deposit at Kasiya is a unique example of a residual placer deposit. Unlike traditional placers, where heavy minerals are transported and concentrated by high-energy processes such as river action, the Kasiya deposit formed in situ. It resulted from the weathering of the primary paragneiss host rock, which led to the concentration of heavy minerals like rutile in place. Graphite within the same paragneiss unit is similarly of interest for its industrial applications, particularly in modern technologies such as batteries and lubricants (Sovereign Metals, 2019).

(mica).

CHAPTER 3: METHODOLOGY

This methodology is designed to systematically address the research objectives, integrating field-based sampling, laboratory analyses, and data driven interpretation. The approach aligns with the international standards, e.g. ASMT, ISO, and priorities productivity, accuracy, and relevance to industrial applications.

STUDY DESIGN



3.1: DESK STUDY

The primary objective of this stage was to gain a comprehensive understanding of the mineralogy, petrography, and geochemistry of flake graphite deposits. This involved reviewing the literature of the study area to identify and compile the existing studies related to flake graphite deposits, mineralogy, petrography and geochemistry. It also involved identifying the key findings, techniques and analytical methods used in the studies. Additionally, the study aimed to synthesize key findings from previous works to establish a foundation for further investigation. It involved examining a broad range of studies to identify the most relevant techniques and analytical methods utilized in characterizing flake graphite deposits.

The review process emphasized identifying gaps in the current body of knowledge and determining trends in geological, mineralogical, and geochemical investigations. Advanced analytical technique such as thin sectioning and imagej software were explored, as these have proven to be pivotal in examining the microstructure and compositional characteristics of graphite deposits (Smith et al., 2015; Johnson and Lee, 2018). Additionally, geochemical analysis methods like Inductively Coupled Plasma Optical Emission Spectrometry (ICP-OES) and XRF were evaluated for their role in determining trace elements within flake graphite (Brown et al., 2020). These techniques provided valuable insights into the genesis and economic potential of graphite deposits

3.2: FIELD WORK AND SAMPLING

The objective of this stage was to collect representative samples, to capture the deposit's spatial, lithological, and structural variability.

3.21. Step 1: mapping

Geological mapping is the process of creating maps that display the types and distribution of rocks and sediments in a specific area (USGS, 2022). The geological mapping of the study area was conducted using differential GPS (Trimble TS5) and Geographic Information Systems (GIS) to accurately delineate lithologies and structural features. The mapped lithologies included graphitic schist, quartzite, amphibolite, and other rock types, while structural features such as folds, shear zones, and lineaments were carefully documented. The integration of GPS data with GIS allowed

for precise spatial analysis and visualization of geological units and structures, facilitating the creation of high-resolution geological maps.

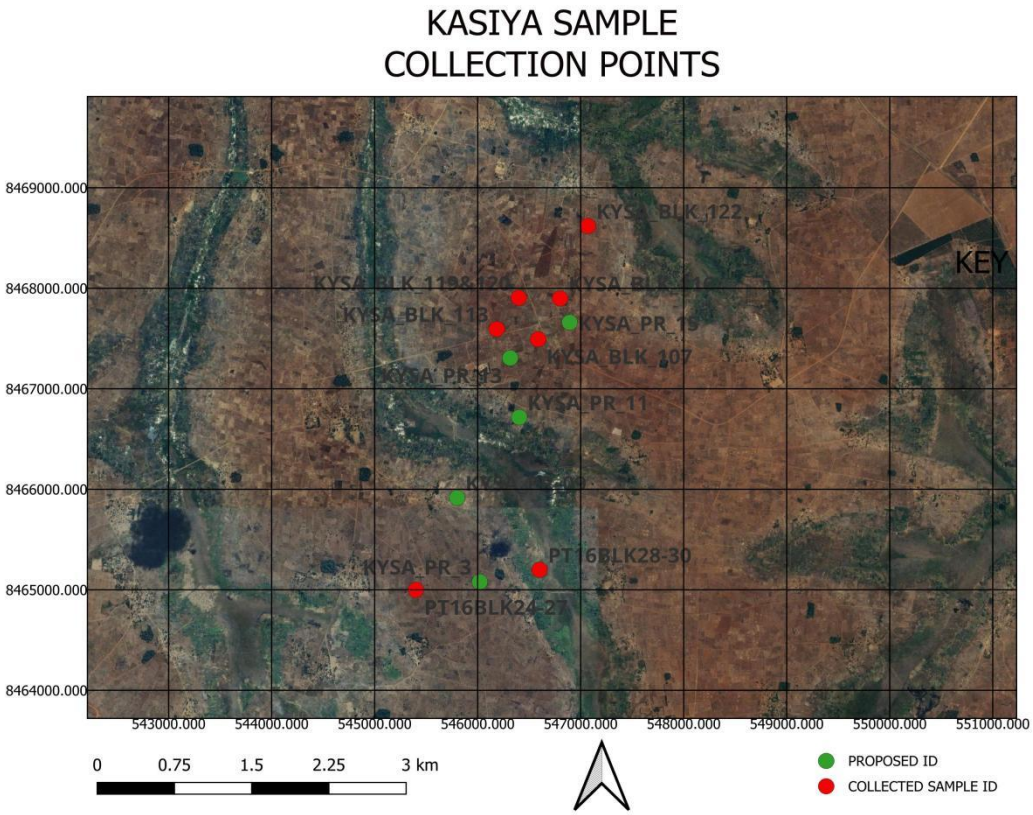
Figure: showing mapping using TS5



Table 1: Sample collection points

SAMPLE ID	East	North	RL	GPS TYPE
KYSA024 To 025	545400.252	8465000.166	1167.184	DGPS
KYSA028 To 031	545600.128	8465200.512	1168.533	DGPS
KYSA_107	546587.334	8467493.313	1170.955	DGPS
KYSA_113	546184.946	8467595.15	1165.55	DGPS
KYSA_116	546800.297	8467899.672	1167.481	DGPS
KYSA_119 & 120	546398.705	8467905.989	1166.274	DGPS
KYSA_BLK_122	547070.751	8468620.32	1156.04	DGPS

Figure 4: Kasiya sample points map



3.22. Step 2: sampling strategy

In Kasiya, graphite occurs as a co-mineral alongside rutile, both of which are believed to have formed through the metamorphism of the parent rock that originally hosted the minerals. Rutile concentrations are higher in the upper layers, decreasing with depth, while graphite concentrations increase with depth.

To target these deposits, sampling was carried out between depths of 6 to 12 meters, extending to 18 meters in cases of poor recovery. A spiral auger was used for sample collection, with intervals of 200 meters between each sampling point to represent the ore deposit. A total of 15 samples were collected from 15 holes, including three duplicate samples for quality control and assurance. Additionally, one blank sample was used for machine calibration and quality assurance purposes. Duplicate samples, blank samples, and certified reference materials were utilized to ensure precision and validation.

Table 2: field observations and geology

A	B	C	D	E	F	G	H	I	J	K	L	M	N	O	P	Q	R	S	T
SAMPLE ID	HoleID	From	To	WEATH	LITH1	LITH2	Colour	Texture	GRA_pc	Flk_Size	Flk_Shape	Flk_Dist	KY_pc	MUSC_pc	BIO_pc	FEOX_pc	Qtz_pc	OS_pc	Moisture
PT16BLK00024	KYSA024	0	0.5	SOIL	SOL		DBR	CG	0				0	0	0	6	25	20	DRY
PT16BLK00025	KYSA025	0.5	1.42	FERP	FERP		DRDBR	CG	0				0	0	0	10	25	20	DAMP
PT16BLK00026	KYSA026	1.42	2	FERP	FERP		DBR	CG	0				0	0	0	10	25	20	DAMP
PT16BLK00027	KYSA027	2	3	MOTT	GNS		DGNBR	CG	0				0	3	0	6	20	15	DAMP
PT16BLK00028	KYSA028	0	1	SOIL	SOIL		BR	CG	0				0	0	0	12	20	25	DRY
PT16BLK00029	KYSA029	1	2	FERP	FERP		RD	CG	0				0	0	0	14	25	20	DAMP
PT16BLK00030	KYSA030	2	3	FERP	FERP		RD	CG	0				0	0	0	12	25	20	DAMP
PT16BLK00031	KYSA031	3	4	FERP	FERP		CRBR	FRI	0				0	0	0	12	20	15	DAMP
KYSA_BLK_107	KYSA107	12	18	SAPL	LGNS		GNGY	FRI	5	COR	EQG	NOR	1	6	2	8	25	20	WET
KYSA_BLK_113	KYSA113	12	15	SAPL	LGNS		YEBR	FRI	4	COR	EQG	NOR	0	2	0	6	30	25	DAMP
KYSA_BLK_116	KYSA116	8	10	PSAP	LGNS		YEBR	FRI	4				0	8	2	8	25	15	DAMP
KYSA_BLK_119	KYSA119	6	13	PSAP	MGNS		LYEGY	FRI	2.5	COR	EQG	NOR	0	8	1	5	25	20	WET
KYSA_BLK_120	KYSA120	13	18.5	SAPL	MGNS		DYEGY	FRI	3	COR	EQG	NOR	0	8	2	4	20	15	WET
KYSA_BLK_122	KYSA122	4	8	MOTT	MGNS		YEBR	CG	1	FIN	EQG	NOR	0	5	0	8	30	25	DAMP

Table 3: Field Observation and Geology Description

PROFILE	DEPTH IN METERS	WEATHER	TYPICAL GRAPHITE	GEOLOGICAL DESCRIPTION
SOIL	0 To 1	TOP SOIL	0.1 To 0.5%	Top soil: reside soil including cultivated/cropped soil. Predominantly sandy clay, may contain grips and angular pebbles strongly enriched in rutile and kyanite, strongly depleted in graphite.
FERP	1 To 4	FERRUGINOUS PEDOLITH	0.5 To 2%	Ferruginous sandy with some clay. May locally contain variably cemented layers that tend towards a duricust, though where present is always less than 1m thick. Strongly enriched in rutile and kyanite, strongly depleted in graphite. Fine graphite flake size. Significant volume loss in this zone during the weathering process.
MOTT	4 To 6	MOTTLED ZONE	1 To 5%	Ferruginous rich and less ferruginous clay+quartz rich mottled colouring. In-situ chemical weathering of clay gangue

				minerals with graphite remaining inert. Primary fabric (ie foliation) may be partialy destroyed. Generally medium graphite flake size. Moderate rutile enrichment, moderate graphite depletion. Some volume loss in this zone during the weathering process.
PSAP	6 To 8	PALLID SAPROLITE	1 To 10%	Pale saprolite dominated by clay and quartz gangue mineralogy (i.e. same as SAPL). Has same graphite grade distribution as SAPL. Generally coarse graphite flake size. No rutile depletion or enrichment. No graphite depletion
SAPL	8 To 25	SAPROLITE	1 To 10%	In-situ, strongly chemically weathered bedrock, with a clay-quartz quartz gangue mineralogy. More than 20% of weatherable-minerals(feldspar/mica/sulphides) altered. Primary fabric of bedrock (i.e. foliation) retained. Generally coarse graphite flake size. No rutile depletion or enrichment. No graphite depletion or enrichment.

3.3 SAMPLE PREPARATION

The samples were prepared at SSL lab. The samples were first dried, weighed their initial weights, recorded and screened using mechanical screening machine, and later desliming.

3.31. Sample crushing and drying

Samples from the field were sun-dried at the pre-processing lab in Airwing lab. Each sample with sample ID tag were placed in drying trays for 3 hours and crushed to fine particle sizes. This was done to remove excess moisture content of the samples. They were then placed in sample bags which a recorded Hole ID and meter number. The samples were logged and weighed. Figure A1

3.32. Sample composing

Compositing involves combining two or more sub-units of a sample in order to make a representative sample. This is often done to reduce the time taken and cost of sample processing. Samples were composited according to their weathering boundaries, i.e., soil, FERP, MOTT, PSAP, and SAPL. After weighing the samples, they were split using a riffle splinter (50-50 splinter) into 2kg composite sample. This splints the sample into two equal halves enabling homogeneous concentration of the samples. The sample IDs were written on the sample bag and ticket IDs. Figure A2

3.33. Sample Screening

This involves separating samples based on the size of particles of samples. After the sample initial weight was recorded, it was soaked for overnight to soften and break the soil bonds and rocks. The drum roller was used to liberate the samples. The machine separated the particles into three sizes, +2mm, 600μm and 45mμ. Each fraction discharged through its separate port.

3.34. Desliming

With the help of water pressure generated from water pumps, +45μm particles of the sample were transferred to the other screen for slimes removal (desliming). the roller drums cleaned the sample as it circulates. The cleaned +45μm fraction was then collected and dried ready to be run on the Wilfley shaking table. Figure A3

After oven drying, the samples were splinted into 500g using a min riffle splinter. The scale used to measure the weights was ULTRA SCALE WALVESBEY. First samples from each hole were send for flotation, the second samples were taken as raw samples, in cases of duplicates, the third sample was taken and the last 500g sample was scored for future references.



3.35. **Froth Flotation samples**

The graphite flotation process is a mineral beneficiation technique designed to separate graphite from associated impurities, such as silicates, sulfides, and other gangue minerals, using its hydrophobic nature.

The samples containing floats and +600μm to 1mm were collected. The initial weights of the two samples, (floats and +600μm to 1mm) were known and used to make 500g composites. The formula used to make the composite of 500g from know weights of the two samples was;

$Float = \frac{FW}{Total\ W}$×500g $\qquad +600\mu m - 1mm = \frac{(+600\mu m - 1mm)}{Total\ W}$×500g

These weights were then added to make a final composite weighing 500g.

For flotation process, I used Denver flotation machine.





3.4. LABORATORY TECHNIQUES

The objective of this step was to characterize mineralogy, texture, geochemistry, and graphite properties. It involved flotation, thin sectioning, geochemical tests, and mineralogical tests.

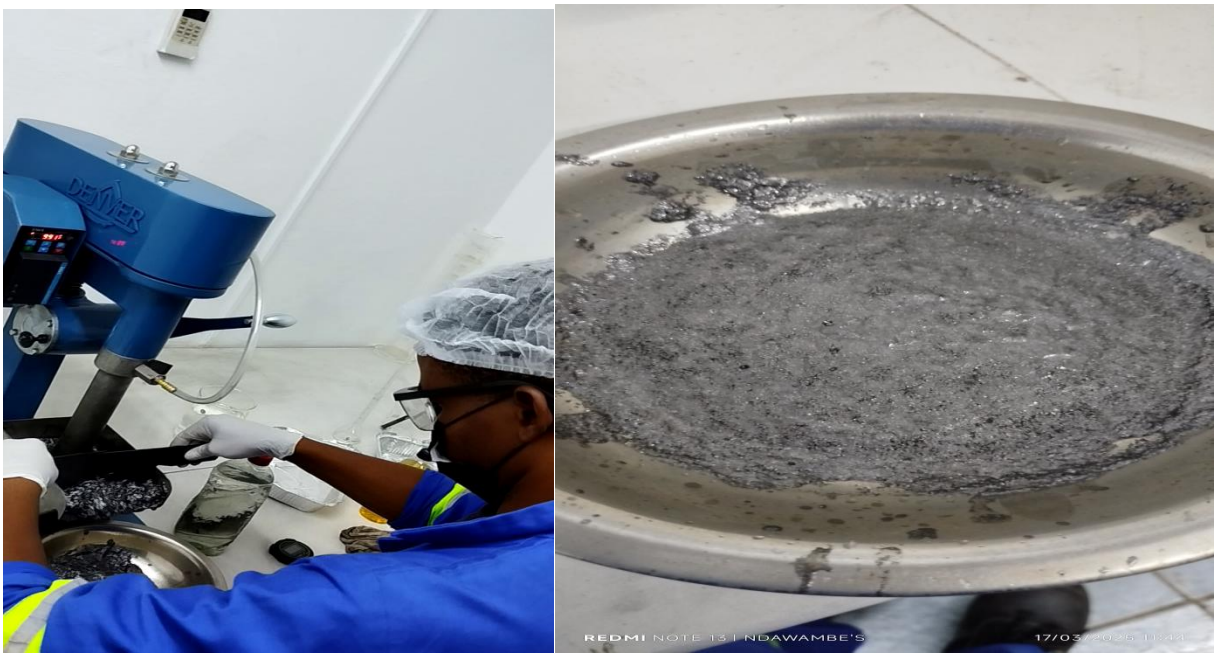
3.41. Froth Flotation

Graphite froth flotation is a specialized method designed to extract and concentrate graphite from its ore by exploiting the differences in the mineral's surface properties. This process plays a crucial role in industries reliant on high-purity graphite for applications such as batteries, lubricants, and refractories.

The procedure requires a variety of equipment and materials to ensure efficiency and accuracy. Key tools include the Denver flotation machine, which is essential for generating the froth, frothers to stabilize the bubbles, pH meters for precise acidity or alkalinity control, filters for separating solids and liquids, collectors to enhance the hydrophobic properties of graphite, scraps for operational adjustments, and flotation cells that serve as the primary site for the separation process. Additional tools, such as a compressed air source, volumetric flasks, sample trays, laboratory funnels, and notepads, support the accuracy and documentation of the procedure.

At SSL Laboratory in Lilongwe, Malawi, this comprehensive froth flotation process was conducted with precision and adherence to quality standards using the company's standard operation procedure. The concentrated graphite was then oven-dried to eliminate residual moisture, ensuring its readiness for industrial applications. Once dried, the material was packaged into sample bags, each bearing a unique sample ID tag to maintain the integrity of records and facilitate traceability for subsequent analysis

Figure showing flotation



3.42. Petrography

Petrographic analysis is the study of the mineralogical composition and texture of the rock through the examination of thin sections under a polarizing microscope. This method allows geologists to identify minerals, assess their relationships, and interpret the geological history of the rock (Mason,2020). Thin sections, typically about 30 micrometers thick, are prepared from the rock samples and mounted on a glass slides, enabling detailed observation of the mineral characteristics such as crystal shape, size, and alteration (Smith & Jones, 2019).

In petrographic analysis, the use of the thin sections is crucial as it provides a clear view of the rock's internal structure through interference of external factors. By utilizing polarized light, geologists can discern optical properties of minerals, such as birefringence and pleochroism, which are essential for accurate mineral beneficiation (Brown, 2021). this technique not only aids in recognizing individual minerals, but also helps in interpreting the rock's formation processes, including sedimentary, igneous, and metamorphic environments (Williams, 2022). Thin section analysis can reveal important geological information, such as grain size distribution, porosity, and the presence of specific textures like filiation or layering. These details can provide insights into past environmental conditions and tectonic settings.

Samples with IDs KYSA_24, KYSA_028_KYSA_107, KYSA_BLANK, and KYSA_120 was prepared for thin section using petrographic techniques. The blank sample was used for quality control and assurance. This was done at Zomba Geological Survey Department. The photo shooting was done at University of Malawi.

3.43 Steps in Thin Sectioning

Impregnation: Each sample was impregnated with a polyester resin, to stabilize its structure. This resin was allowed to cold-cure in a ventilated cabinet for 7 days.

Hardening: Once the resin was set, each sample was placed in an oven for hard curing at low heat. This ensured the sample is solidified and ready for cutting.

Cutting and Grinding: The hardened sample was cut into thin slices using a diamond saw. These slices were then ground to 30μm using specialized grinding machines.

3.44. Mineralogical characteristics

Mineralogical analysis of graphite focuses on characterizing its crystal structure, chemical composition, physical properties, and textural features to determine its quality, origin, and suitability for industrial applications.

3.5 Geochemical Analysis

3.51. X-Ray Fluorescence (XRF)

The main objective for this test was to determine the chemical composition of graphite raw samples, and pure samples. This method works by exposing a sample to high-energy X-rays, which excite the atoms within the material. This excitation causes the atoms to emit secondary (or fluorescent) X-rays that are characteristic of their specific elements. This test took place at the University of Malawi.

3.52. Inductively Coupled Plasma Mass Spectrometry (ICP-OES)

This highly sensitive technique was used to analyze trace elements. It enabled the detection of low concentration of elements, like Cu, Ni, As, to identify geochemical anomalies and providing a comprehensive view of the mineral composition of the graphite.

CHAPTER 4: RESULTS AND DISCUSION

4.1. Petrography

4.1.1 thin sections

Each thin section sample was examined using PPL and XPL under polarized light at University of Malawi. Polarized light microscope was used to identify the mineral assemblages, e.g graphite, biotite, quartz. The textures like flake alignment, foliation, deformation features were documented. The magnification used was ×10 in both PPL and XPBL. For interpretation, I used imagej software.

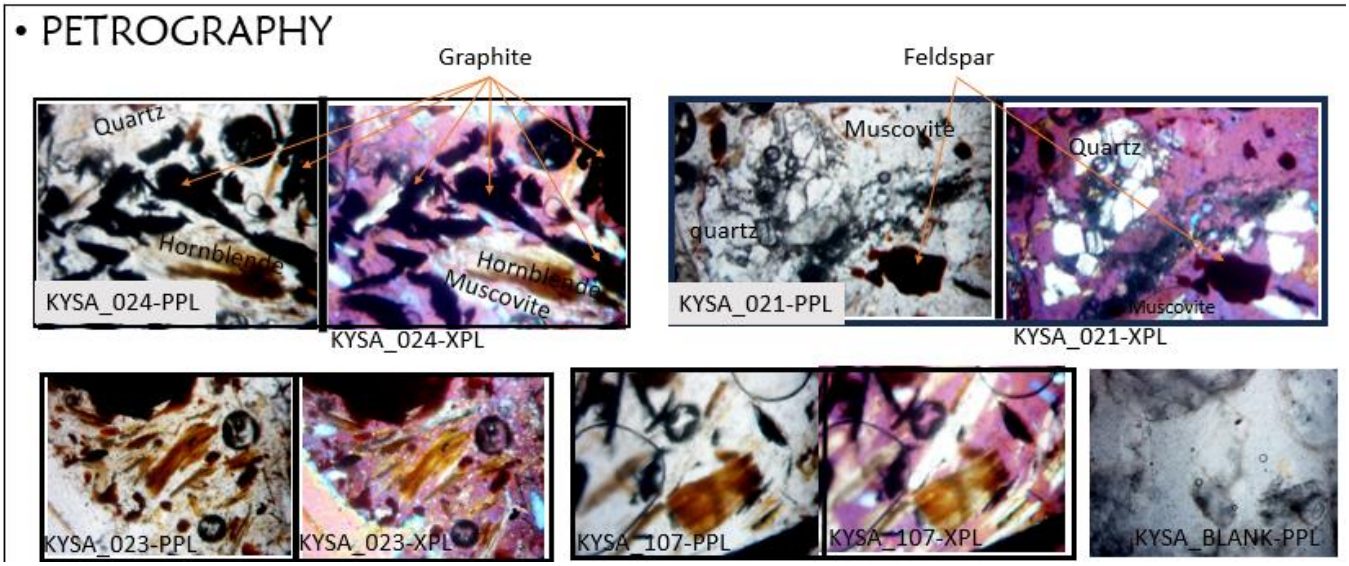


Fig: graphite and elemental associations

SAMPLE ID	GRAPHITE PRESENT	DOMINANT MINERALS	ROCK TYPE	METAMORPHIC GRADE	PROTOLITH
KYSA_024	YES	Quartz Feldspar Mica	Graphitic Geiss/schist	Greenschist amphibole	Mudstone-silkstone mix
KYSA_028	YES	Quartz Feldspar Mica	Graphitic Schist	Greenschist amphibole	Organic shale
KYSA_BLANK	NO	Quartz	Pure Quartz (possible contamination)	Medium,M	
KYSA_107	YES	Quartz Feldspar	Graphitic metasedimentary rock	Greenschist	Carbon rich metasedimentary rock

		Mica			
KYSA_120	YES	Quartz Feldspar Mica	Graphitic mica schist	Greenschist	Graphite bearing metapelite

Mineral	Estimated %		
Quartz	30-35%	Plagioclase	25-30%
K-feldspar	5-10%	Biotite	10-15%
Muscovite	5-8%	Graphite	5-10%
Opaques	<2%	Accessories	<2%

4.12 Common Flake Morphology

Shape: The flakes are irregularly shaped, with some showing elongated, needle-like forms and others appearing lobate or angular. Alignment of Platy Minerals: The thin sections reveal that more than 50% of the minerals, including graphite flakes and micas, are aligned parallel to each other. This alignment contributes to the rock's fissility, allowing it to split into thin flakes or slabs.

Grain Size and Texture: The graphite flakes exhibit fine to medium grain sizes and are elongated, consistent with the characteristics of schistosity. The presence of these well-aligned, elongated minerals indicates a strong foliation developed under directed pressure during metamorphism.

Metamorphic Grade: The mineral assemblage and textures suggest that the rocks have undergone medium- to high-grade metamorphism, likely within the amphibolite facies. This is supported by the presence of minerals such as biotite and muscovite, which are stable at these metamorphic conditions.

Orientation: The graphite flakes exhibit a preferred alignment parallel to the foliation, indicating deformation during metamorphism.

4.13 Overview of Thin Sections

Graphite: Present as fine to medium-sized flakes, often aligned along foliation planes, indicating recrystallization under directed pressure.

Quartz and Feldspars: Dominant in the matrix, suggesting a siliceous protolith.

Micas (Biotite and Muscovite): Abundant and aligned, indicative of medium- to high-grade metamorphism.

Accessory Minerals: Presence of opaque minerals, possibly sulfides, and occasional amphiboles.

Foliation: Well-developed, with graphite and mica alignment, pointing to regional metamorphic influences.

Grain Size: Graphite flakes range from 50–150µm, consistent with flake graphite formed under high-grade conditions.

4.14 Petrographic interpretation

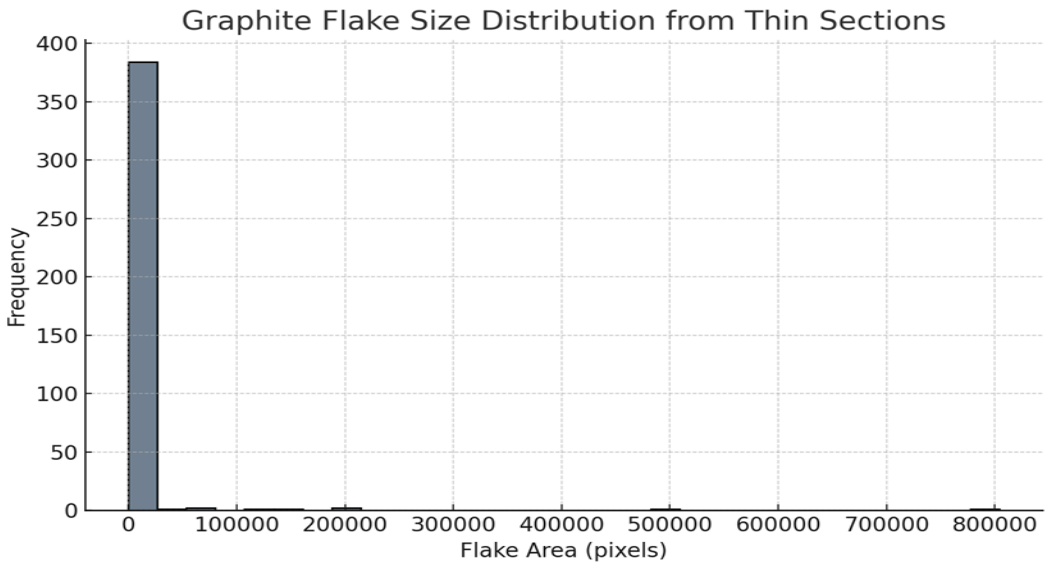
Petrography was used to identify mineral composition, analyze rock texture, and classify the rock sample. The Kasiya flake graphite schist is primarily composed of graphite, quartz, mica muscovite, and mica biotite and feldspar. These minerals are small to medium, and at some holes, course-grain and sorted into parallel to alignment foliation textures (fig)The texture is granoblastic to lepidonlastic due to the presence of micas and graphite. The schistosity is characterized by a well-developed planar fabric defined by the parallel alignment of platy minerals, primarily graphite and micas (biotite and muscovite).

The metamorphic grade of Kasiya ore is medium grade due to the presence of biotite, muscovite, undulose quartz, and stable graphite. The origin is likely metamorphosed sedimentary protolith rich in organic matter, e.g., carbonaceous shale and mudstone. The petrographic analysis of the Kasiya samples shows a mix of rocks, including metamorphosed graphitic pelites and quartz-rich schists. These rocks were transformed by regional metamorphism under conditions ranging from greenschist to amphibolite facies. Similarly, the KYSA samples consist of metasedimentary rocks, primarily graphitic schists and semi-pyelitic gneisses, which originated from organic-rich mudstones and siltstones. The presence of dispersed graphite in most samples suggests they were deposited

in a low-oxygen sedimentary basin. Later, they experienced regional metamorphism, possibly connected to the Pan-African Orogeny. Additionally, the observation of dark minerals in blank thin sections might point to minor contamination during the thin sectioning process.

4.15 Flake Size Distribution

Mean flake size	6,193 pixels2
Median size	84 pixels2
Maximum Size	804,001 pixels2
Minimum size	20 pixels2



The distribution of graphite flakes ranges from 20pixels^2 to 804,001pixels^2, with a median size of 84 pixels^2. The flake size distribution suggests a wide size distribution, characteristic of flake graphite formed under varying metamorphic conditions or deformation

4.2 X-Ray Fluorescence XRF Results

4.21 Mineralization process

The objective was to understand the mineralization processes that have led to the concentration of graphite and other associated minerals at the Kasiya flake graphite deposit, and identify the elemental impurities associated with Kasiya flake graphite. To analyze the results and draw conclusions regarding the mineralization of graphite and associated minerals at the Kasiya rutile deposit, we consider the geological descriptions, ICP-OES, and XRF data alongside knowledge of graphite mineralization processes.

Kasiya graphite flake concentration increases with depth, such that topsoil and colluvial soils are enriched in kyanite and rutile and significantly depleted in graphite. With depth, the concentration of graphite increases up to about 5-10% from meters 6 to 25, and strongly depleted in rutile up to about 0.2 to 0.5%.

Figure showing XRF results

ELEMENTAL C	KYSA_024	KYSA_120	KYSA_028	KYSA_107	KYSA_BLANK
MgO Concent	9921	86104	7822	109294	0
Al2O3 Concer	152149	132929	131744	167560	18657
SiO2 Concent	237436	224292	306100	228761	434462
PO2 Concentı	886	2711	1231	1408	0
SO Concentra	1257	3448	2380	6663	143
K Concentrati	4986	33999	8107	32205	0
Ca Concentra	0	0	0	0	0
Ti Concentrat	4769	5716	4341	5334	422
V Concentrati	154	301	151	300	0
Cr Concentra	139	119	91	129	47
Mn Concentr	1185	500	595	728	0
Fe Concentra	97062	35845	55883	40947	819
Co Concentra	0	0	0	0	0
Ni Concentra	162	56	82	222	12

MEAN ELEMENT CONC

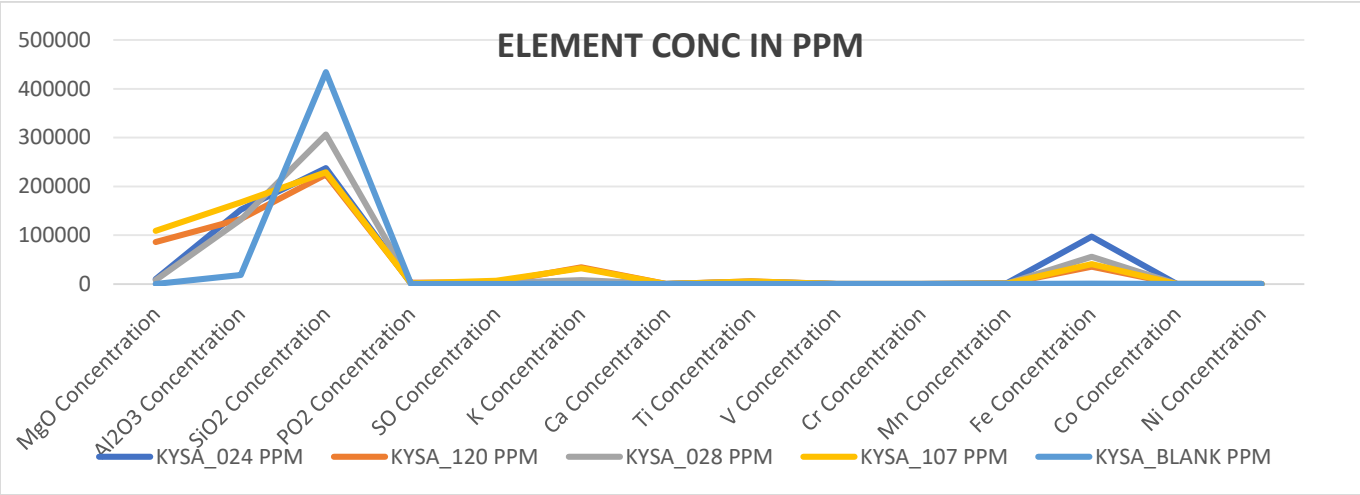


Figure showing elemental concentration of kasiya raw samples

Quartz is notably abundant in all samples, particularly in the blank sample (KYSA_BLANK), confirming its dominance. The flake graphite ores (KYSA_024, KYSA_120, KYSA_107) exhibit lower levels of SiO_2, which can be attributed to the presence of other silicate minerals, such as mica, feldspar, and graphite. High silica and alumina levels mean that liberation of graphite may require significant grinding and flotation stages.

High SiO_2 and Al_2O_3 reflect a quartz-feldspar-rich composition, typical of pelitic or psammitic protoliths. Elevated Fe_2O_3 and MgO suggest the presence of biotite and possible amphibole, supporting medium- to high-grade metamorphic conditions. Moderate CaO and Na_2O Indicate plagioclase feldspar content and potential metasomatic alterations.

Elevated Cr, Ni, and V may point to mafic contributions or fluid interactions during metamorphism. Presence of S, correlates with sulfide minerals observed petrographically, suggesting reducing conditions during metamorphism

4.22 Metasomatic Influences

Fluid Activity: The presence of elements like Cr, Ni, and V, along with S, implies fluid-mediated element mobility, contributing to graphite formation and mineral assemblage modifications.

Redox Conditions: Reducing environments, as indicated by sulfide presence, would favor the stabilization and preservation of graphite during metamorphism

4.23 Major Elements and Host Matrix

SiO_2: Extremely dominant . Indicates a silicate-rich host rock, likely quartz or quartz-rich metasediments (e.g., quartzite, graphitic schist).

Al_2O_3: High Presence of aluminous minerals such as kaolinite, muscovite, or feldspars. Suggests a pelitic origin or clay-rich layers.

Fe : Very high Strongly implies the presence of iron-bearing silicates (e.g., biotite, chlorite) or oxides (e.g., magnetite). Also common in metamorphosed sediments.

MgO : Suggests magnesium silicates like chlorite or serpentine. Can also be linked with talc in high-grade metamorphic terrains.

K: Moderate May point to K-feldspar or micas (especially muscovite/biotite), common in gneisses or schists.

Ti: Minor but relevant. Likely from rutile which are heavy minerals often associated with metamorphic rocks.

4.24 Accessary/Trace Elements

SO, PO_2 Possibly from sulfide minerals (e.g., pyrite) and phosphates (e.g., apatite), indicating hydrothermal or metamorphic processes.

V, Cr, Ni are moderate .Often found in ultramafic or mafic environments; the presence of Cr and Ni supports the idea of a metamorphic origin, possibly with mafic inputs or retrograde alteration.

Trace Mn suggests presence of minor garnet or spessartine, or manganese oxides.

Ca is absent confirming lack of carbonate minerals (e.g., calcite, dolomite). Implies this is not a marble-hosted graphite deposit.

Absentof cobalt minerals is due to the fact that it is not associated with metamorphic graphite ores.

4.25 Petro-genetic Implications

The data supports a metasedimentary origin, with graphite hosted in high-silica, alumina-rich lithologies.

Absence of Ca eliminates carbonate lithologies; presence of Fe, Mg, K, and Al suggests a high-grade metamorphic setting-potentially graphitic schists or gneisses.

Elevated Cr, V, and Ni may hint at interaction with or derivation from ultramafic sources or reflect a higher metamorphic grade with element mobility.

4.26 Mineralogical Indicators (Inferred from XRF)

Likely gangue minerals: Quartz, muscovite, biotite, feldspars, chlorite, rutile/ilmenite, and minor sulfides.

Ore mineral: While carbon (graphite) is not detected via XRF, the mineralogical context is consistent with flake graphite formation under regional metamorphism.

4.27 Implications for Beneficiation

High silica and alumina levels mean that liberation of graphite may require significant grinding and flotation stages. Low Ca and absence of reactive carbonates simplifies the chemical processing. Trace metals do not suggest significant economic by products but could affect tailings composition.

4.3 ICP-OES

Sample ID	**KYSA-BLK-107 A Conc 1**	**KYSA-BLK-107 B Conc 1**	**KYSA-BLK-120 Conc 1**	**KYSA-BLK-28 A**	**BLANK**
Aluminium, mg/kg	4,517.0	3.,412.0	31,129.0	7,415.0	16.3
Potassium, mg/kg	889.0	692.7	616.6	5.61	253.2
Sodium, mg/kg	5,434.0	462.5	343.4	561.3	316.4
Iron, mg/kg	16,483.3	14,678.3	14,177.5	561.3	3.14

Manganese, mg/kg	4.62	404.4	367.5	2,070.5	562.1
Calcium, mg/kg	7.34	680.5	654.0	11.28.0	126.91
Magnesium, mg/kg	939.2	672.3	654.0	1,128.0	0.8
Chromium, mg/kg	10.3	8.5	6.3	16.8	0.36
Nickel, mg/kg	35.57	30.24	7.42	27.5	156

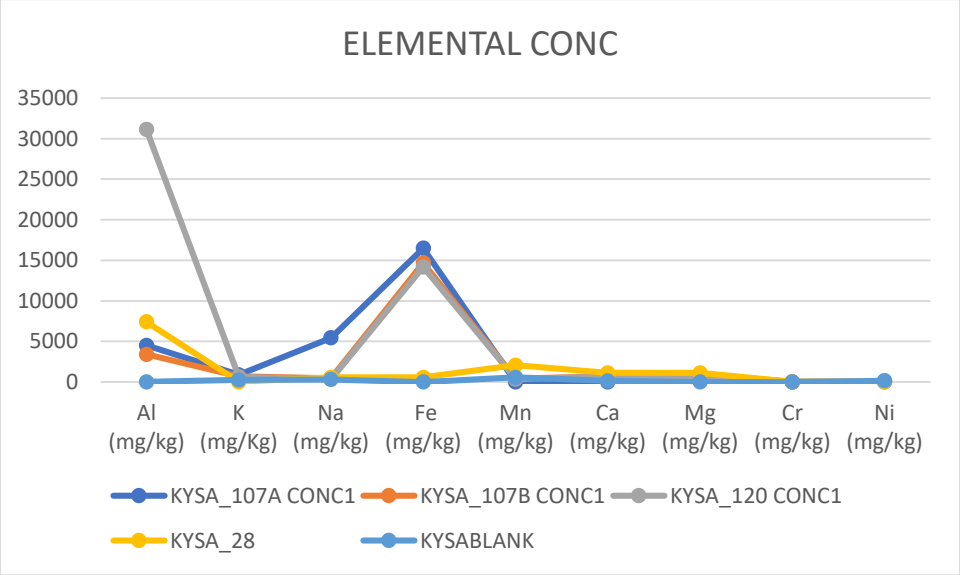


figure showing elemental concentration in graphite samples

The elemental concentrations measured in milligram per kilogram includes aluminum, potassium, sodium, iron, manganese, calcium, magnesium, chromium and nickel, with iron dominating in three samples. High concentration of iron in samples indicates presence of biotite, magnetite or other iron oxides. There is a peak aluminum concentration in KYSA_120, with some significant concentration from all but one sample. This can indicate aluminosilicates such as feldspar and micas. Sodium and potassium supports plagioclase and K-feldspar/muscovite. The magnesium and

manganese levels correspond with biotite and garnet/chromite components. Nickle and chromite levels suggests trace sulfide phases or mineral inclusions, confirming subtle metasomatic influence.

These results directly align with the petrographic thin section results. Quartz, feldspar, muscovite, and biotite were confirmed petrographically, and their presence is strongly supported by Al, K, Fe, and Mg content. Graphite, seen in thin section as flaky, isotopic, and often aligned with foliation, is consistent with the absence of interference elements, supporting high purity flake graphite. The texture and mineral alignment suggest medium grade regional metamorphism, possibly amphibolite faces, aligned with mineral stability (biotite, muscovite graphite)

The flake graphite at Kasiya is hosted in biotite-muscovite-quartz-feldspar gneisses and schists, derived from carboniferous politic sedimentary protoliths. The geochemical profile reflects metamorphic recrystallization of original clay-and organic-rich sediments. Medium grade metamorphism allowed for the preservation and enlargement of graphite flakes, enhancing their economic potential. The presence of Ni, Cr, and Mn may indicate minor metasomatic input, possibly from circulating metamorphic fluids, but not enough to compromise purity. The data confirms that graphite is of high purity with limited impurities, making it suitable for high-end applications

4.31 Metasomatic Activity

The alignment of graphite along foliation planes indicates dynamic recrystallization under stress-typical of regional metamorphism. The overgrowth textures in chlorite and mica on graphite suggests fluid-induced mineral replacement, characteristic of metasomatic reactions. Granoblastic textures in quartz-feldspar-mica assemblages further supports recrystallization.

In relation to mineralogy, presence of chromite, sericite, and feldspars in otherwise carbon-rich graphitic rocks implies chemical alteration by fluids. The ICP-OES and XRF show elevated levels of Fe, Al, Ca, K, and Mg elements that are mobile in metamorphic fluids, further supports metasomatic activity.

The somatic source is likely driven by CO_2 and H_2O rich metamorphic fluids, possibly introduced during regional metamorphism or tectonic events. The presence of alkali and alkaline earth

elements like Na, K, Ca, and Mg, supports the involvement of hydrothermal or metamorphic brines. Metasomatic fluids inhances recrystallization, mineral transformation, and flake development.

CHAPTER 5: CONCLUSION AND RECOMMENDATIONS

5.1 CONCLUSION

This study presents an integrated mineralogical and petrographic analysis of graphite-bearing rocks from the Kasiya region, aimed at characterizing the flake graphite occurrences, their host mineral assemblages, and the geochemical environment of formation. Thin section petrography, combined with elemental analysis via XRF and ICP-OES, provides a comprehensive understanding of the deposit's mineralogical composition, textural relationships, and metamorphic evolution.

Petrographic analysis of thin sections reveals that the graphite is hosted predominantly in medium- to high-grade metamorphic rocks, specifically graphitic biotite-muscovite-quartz-feldspar gneisses and schists. The texture is primarily granoblastic to lepidoblastic, with evidence of recrystallization and mineral alignment indicative of regional metamorphism. Graphite occurs as fine to coarse flakes, often intergrown with biotite and muscovite, and aligned parallel to foliation planes, suggesting syn-metamorphic formation. Other common minerals include quartz, plagioclase, K-feldspar, and accessory phases such as zircon and opaques (likely oxides and sulfides).

Under plane and cross-polarized light, graphite appears as dark, flaky, isotropic grains, and its spatial association with mica minerals supports its derivation from carbon-rich sedimentary protoliths, such as black shales. The presence of undulose extinction in quartz and partial alteration in feldspar further indicates moderate to high degrees of deformation and metamorphism.

XRF results confirm the presence of major and trace elements consistent with the observed mineral assemblage. High Fe concentrations correspond to biotite and possible oxides, while trace levels of Ni, Zr, and Cd suggest the presence of minor accessory or sulfide minerals. Notably, the detection of Zr aligns with the presence of zircon in thin section, while Na supports plagioclase feldspar as a significant phase. Although carbon itself is not detected by XRF due to instrumental

limitations, the absence of interference from light elements and the associated mineral phases support the graphite interpretations.

ICP-OES data (referenced) further validate the bulk composition, indicating elevated Fe, Al, and Si, consistent with the presence of aluminosilicates (micas and feldspars) and quartz. Low concentrations of base and precious metals affirm that the deposit is primarily of industrial interest for its graphite, rather than for economic sulfides.

Taken together, the data indicate that the graphite at Kasiya formed through the metamorphism of a carbonaceous sedimentary protolith, with the development of flake graphite occurring in response to medium- to high-grade metamorphic conditions, likely in the amphibolite facies. The preservation of flake morphology and the absence of significant retrograde alteration suggest a relatively stable metamorphic environment, enhancing the quality and economic potential of the graphite.

In conclusion, the Kasiya flake graphite deposit is of metamorphic origin, hosted in aluminous silicate-rich gneisses and schists, and characterized by well-developed, disseminated graphite flakes with favorable crystallinity and associations. This understanding provides a solid geological basis for evaluating the deposit's resource potential and guiding future exploration and beneficiation strategies.

5.2 RECOMMENDATION

This study used limited techniques to unveil the whole detailed mineralogical and petrographic analysis. Applying more suitable techniques like XRD, SEM, ICP-MS would enhance the understanding of the deposit's mineralogy and petrography. This paper does not contain all planned data, including pictures due to the incident where I lost my laptop to thieves just few days before submitting the dissertation.

REFERENCES

Benchmark Minerals. (2023). Graphite Market Trends and Forecasts. Benchmark Mineral Intelligence

Brown, A., et al. (2016). *Traditional applications of graphite*. Retrieved from https://en.wikipedia.org

Britannica. (n.d.). Karoo Supergroup. Retrieved from https://www.britannica.com/

Bullock, R., & Morgan, J. (2015). Graphite Genesis in Metamorphic Terranes. Journal of Geoscience Research, 12(3), 45-62.

Chikafumbwa, R. (2022). *Sustainable Mining in Malawi*: Opportunities and Challenges. Journal of African Resource Studies, 18(3), 45-62.

DeBruyn, I., Hunter, R., & Key, R. M. (2015). *Geology of the Ubendian Belt in Malawi*. Journal of African Earth Sciences, 105, 1–14.

Deutsche Rohstoffagentur (DERA). (2020). *Supply and demand of natural graphite.* Retrieved from https://www.deutscherohstoffagentur.de/DERA/DE/Downloads/Studie%20Graphite%20eng%202020.pdf?__blob=publicationFile&v=3

Doe, J. (2020). The Global Shift to Renewable Energy: The Role of Minerals. Energy Publishing House.

European Minerals Yearbook. (2023). Graphite resources and production in Europe. Retrieved from https://minerals.eu

International Energy Agency. (2024). Critical minerals and graphite demand in energy storage. Retrieved from https://iea.org

International Energy Agency (IEA). (2023). Critical minerals and their role in energy transitions. Retrieved from https://iea.org

International Energy Agency (IEA). (2022). Global Battery Materials Supply and Demand Outlook. Retrieved from https://www.iea.org.

Johnson, C., Smith, R., & Bell, T. (2018). Graphite Deposits: *Characterization and Market Trends*. Geoscience Journal, 25(4), 123-140.

Johnson, K., & Walker, W. (2022*). Graphite in fuel cells and Li-ion batteries*. Retrieved from https://pubs.rsc.org

Jones, J. (2018). *Surface energy and sublimation point of graphite*. Retrieved from https://www.academia.edu

Lee, J., et al. (2022). Processes in graphite formation: Metamorphic vs. hydrothermal origins. Journal of Geoscience Research, 45(3), 235–250.

Lee, J., & Kim, C. (2021). Young's modulus of graphite. Retrieved from https://link.springer.com

Meunier, A. (2015). Carbon Allotropes and Their Properties. Carbon Science Journal, 8(2), 123-134.

Meunier, B. (2015). Graphite Science and Applications Noble, G., Aziz, S., & Taylor, J. (2020). Genesis of Graphite Deposits: Insights from Southern Africa. Earth Science Review, 193, 221-235.

McNulty, P. (2021). The Role of Graphite in Renewable Energy Technologies. Energy Materials Journal, 14(2), 89-102.

Palosaari, T., et al. (2020). Structural Characteristics of Graphite. Materials Chemistry Review, 15(4), 89-102.Roskill. (2024). Graphite market and demand overview. Retrieved from https://roskill.com

Puronaho, K. (2018). *Thermal and Electrical Properties of Graphite*. Journal of Materials Science, 33(1), 67-78.

Qi, Y., et al. (2019*). Graphite and Its Allotropes*: A Structural Perspective. Carbon Materials Journal, 14(3), 101-115.

Robinson, D., et al. (2017). Natural vs. Synthetic Graphite: A Comparative Study. Industrial Minerals Review, 22(5), 56-78.

Rosing-Schow, N., et al. (2017). Challenges in Graphite Supply Chains. Resources Policy, 42(2), 34-45.

Roskill. (2024). Graphite market and demand overview. Retrieved from https://roskill.com

Simandl, G., et al. (2015). Graphite Deposits and Their Industrial Applications. Economic Geology, 110(3), 567-589.

Smith, D. M. (2020). Anisotropic conductivity ratio of single-crystal graphite. Retrieved from https://www.researchgate.net

Sovereign Metals. (2025). Kasiya Rutile-Graphite Project Overview. Retrieved from https://sovereignmetals.com.au

Sunkari, M., & Zango, P. (2018). Global Graphite Market Trends. Journal of Industrial Minerals, 19(4), 78-89.

Statista. (2024). Graphite demand globally by application 2025. Retrieved from https://www.statista.com/statistics/452281/graphite-demand-worldwide-prediction-by-application/

Tsunogae, T., Santosh, M., & Asiedu, D. (2021). Gondwana fragmentation and associated magmatic activity: Evidence from Karoo dolerites in southeastern Africa. Precambrian Research, 345, 105–121.

United Nations. (2015). Transforming our World: The 2030 Agenda for Sustainable Development. Retrieved from https://sdgs.un.org/goals.

U.S. Geological Survey (USGS). (2024). Grade and tonnage data for disseminated flake graphite deposits. Retrieved from https://www.usgs.gov/data/grade-and-tonnage-data-disseminated-flake-graphite-deposits

US Geological Survey. (2023). Mineral commodity summaries: Graphite. Retrieved from https://usgs.gov

Wadie, L., Nkomo, P., & Zione, K. (2023). Graphite in Precambrian Terranes: Metamorphic and Hydrothermal Perspectives. Precambrian Research Journal, 287, 34-56

World Bank Group. (2023). Africa's mineral potential: Graphite reserves and mining opportunities. Retrieved from https://worldbank.org

World Bank. (2023). Malawi: Country profile and economic outlook. Retrieved from https://worldbank.org

Zhu, X., et al. (2019). Electronic and crystal structure–property relationship of natural graphite. Retrieved from https://link.springer.com